Effect of wall heat transfer on the dynamics of premixed spherical expanding flames

A. Mouze-Mornettas, H. Keck, Y. Wang, Z. Chen, G. Dayma, C. Chauveau, F. Halter

Effect of wall heat transfer on the dynamics of premixed spherical expanding flames

A. Mouze-Mornettas[a,b], H.Keck[a], Y. Wang[c], Z.Chen[c], G. Dayma[a,d], C. Chauveau[a], F. Halter[a,d]

[a]*CNRS ICARE, Avenue de la Recherche Scientifique, 45071 Orléans Cedex 2, France*
[b]*CERFACS, 42 avenue G. Coriolis, 31057 Toulouse Cedex 01, France*
[c]*SKLTCS, College of Engineering, Peking University, Beijing, China*
[d]*Université d'Orléans, Orléans Cedex 2, France*

Corresponding author: A. Mouze-Mornettas
email: antoine.mouze@cnrs-orleans.fr

Abstract

Premixed laminar flame speed determination is a crucial point since its values are used for the sizing of every combustion systems. In order to measure this parameter, an isochoric combustion method can be used. It consists in measuring the pressure (and possibly other parameters) for a spherical expanding flame. This method allows to get flame speed data for a large scope of important pressures and temperatures supposing an isentropic compression. However, the entirety of the flame propagation process cannot be used to compute the flame speed as heat losses will start to appear as the flame come close the wall, making the isentropic compression assumption invalid. In order to precisely determine when significative heat losses occur, a criterion based on the evolution of the flame preheat zone thickness is described in this paper. The evaluation of this new method is performed using Direct Numerical Simulations for different mixtures (methane with various diluents) at different equivalence ratios and thermodynamic conditions. Finally, the criterion is compared to already existing methods, showing a relatively good accuracy to describe wall heat losses effect on the flame dynamics at high pressure.

Keywords

Heat losses, laminar flame speed, isochoric combustion, spherically expanding flame, preheating zone thickness, high pressure

1. Introduction

Flame speed knowledge is a key parameter for sizing combustion-based systems. It is defined as the propagation speed relative to the unburnt mixture of a steady, laminar, one-dimensional, planar, stretch-free, and adiabatic flame, hereafter referred to as freely propagating flame S_u. At the direct application level, it affects the fuel burning rate, which has a direct impact on the system performance. Hence this is a major parameter to consider during sizing calculations, used in several turbulent flame computation models for CFD. On a more fundamental level, it is an important target for the validation of kinetic mechanisms. Accurate determination of flame speeds at high pressures and temperatures is extremely important for the development of kinetic mechanisms and ensure their validity in the simulation of industrial configurations. Several methods have been developed to experimentally measure the laminar flame speed but most of them allows limited pressure and temperature variation ranges. One of the methods to obtain data at high pressure and temperature conditions relies on a procedure initially proposed by Lewis and Von Elbe [1] . It consists in studying the flame expansion in a fixed volume, method referred here as SEF-CONV for *Spherical Expanding Flame at Constant Volume*. The general idea is to record the pressure evolution over time inside the

combustion chamber in order to evaluate the flame speed S_u. The flame is initiated in the center of the chamber and propagates outwardly till it reaches the walls.

Conversion of the reactants to hot burnt gas across the flame front results in a rapid pressure increase and a corresponding temperature rise in unburnt and burnt gas. The constant volume technique relies on the relation between the instantaneous flame speed, the pressure evolution and the radius history. In other words, in a single test, flame speeds can be obtained for a range of high pressures and temperatures. This makes the study SEF-CONV a widely used method to characterize the laminar flame speed of various fuels in different conditions [2–7].

In order to compute the flame speed knowing the pressure evolution inside the chamber, several assumptions need to be made:

- The pressure P is spatially uniform in the chamber
- Burnt and unburnt gases are considered as an ideal gas
- There are no chemical reactions in the fresh gases
- The flame is perfectly spherical with an infinitesimally thin flame front
- Unburnt gases are compressed isentropically

Based on these assumptions, the following expression of the laminar flame speed S_u relative to the unburnt mixture was derived [3]:

$$S_u = \frac{dR_f}{dt} - \frac{R_0^3 - R_f^3}{3\gamma_u R_f^2 P}\frac{dP}{dt} \tag{1}$$

R_f and R_0 being respectively the flame radius and the inner chamber radius, and γ_u the heat capacity ratio of the unburnt gases. This relation supposes the knowledge of the simultaneous evolution of R_f and P during the flame propagation till it reaches the walls.

Classically, combustion chambers used for SEF-CONV studies do not have any optical access because of the extreme conditions encountered during flame propagation. Hence, R_f needs to be computed using the following relation (P_0 being the initial pressure and x the mass fraction of burnt gases):

$$\frac{R_f}{R_0} = \left[1 - (1-x)\left(\frac{P_0}{P}\right)^{\frac{1}{\gamma_u}}\right]^{\frac{1}{3}} \tag{2}$$

The knowledge of the $x = f(P)$, therefore $R_f = f(P)$, evolution requires a model [3,8]. The pressure dependence of x can be described in many ways depending on the chosen correlation [8].

In order to avoid accuracy issues coming from such models, a new type of combustion chamber was developed. Figure 1 shows a recently developed experimental set up : OPTIPRIME [9] is a perfectly spherical isochoric combustion chamber of 60.85 mm radius with full (i.e. 360°) optical access. Pressure evolution inside OPTIPRIME is acquired thanks to 2 high sensitivity and frequency pressure sensors while a type-K thermocouple allows to assess the initial temperature of the unburnt gases. This is a unique setup, allowing the measurement of the flame radius, the detection of the development of instabilities and the achievement of high pressures (up to nearly 100 bar). The simultaneous access to pressure and radius is unique. Progress has been made on the identification of the limits of data to process to compute S_u, taking into account stretch effects after ignition and wall heat loss at the end of the flame propagation [9].

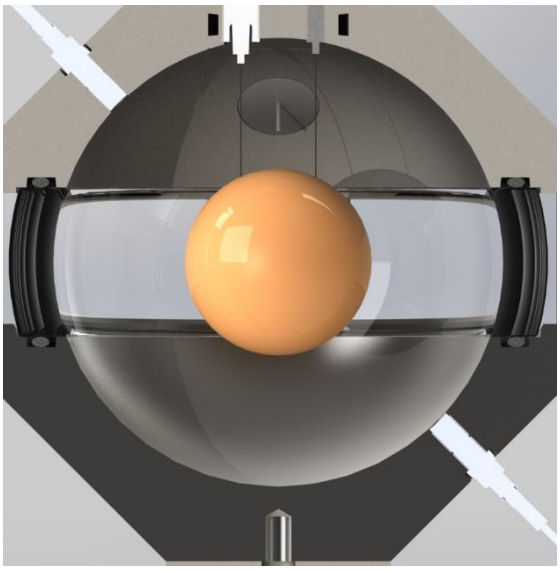

Figure 1: Illustration of the SEF-CONF configuration. The flame corresponds to the orange sphere in the center of the chamber. It is initiated thanks to the two electrodes and propagates outwardly. Two pressure sensors (in white) are diametrically opposed. This system allows the visualization of a large part of the flame untill it reaches the wall.

A limiting factor which needs to be considered when measuring flame speed with the SEF-CONV setup concerns the flame front stability. Gravity effects can modify the flame shape for low flame speed (approximately for S_u< 15 cm s^{-1}). It is also important to consider the modification of the flame surface induced by hydrodynamic and thermodiffusive instabilities. The latter are related to the competition between the molecular diffusion D_m (i.e. mass flux) and the thermal diffusion D_{th} (i.e. heat flux), which can be characterized thanks to the Lewis number Le:

$$Le = \frac{D_{th}}{D_m} = \frac{\lambda_u}{\rho_u C_{p_u} D_m} \tag{3}$$

ρ_u, C_{p_u} and λ_u are the unburnt gas density, heat capacity and thermal diffusivity respectively.

The molecular diffusion considered is the one from the minor species into the rest of the mixture, hence D_{th} evaluation is dependent on the mixture composition. Interestingly, for mixtures with CH_4 as fuel, Le increases with equivalence ratio (φ).

The high stretch levels undergone by the flame during the initial propagation stage allow to keep the flame stable. However, the flame surface may progressively wrinkle as the flame propagates when Le is close to unity, as it is the case for methane/air mixtures. The surface modification leads to a non-spherical flame propagation, hence preventing S_u evaluation. It is mandatory to keep in mind that pressure has also an effect on cells development. Indeed, as the pressure increases, the flame thickness, δ_f, decreases, leading to a thinner flame front that favors the flame destabilization by a hydrodynamic process. This observation is very important since the targeted experimental conditions are high pressure, compatible with industrial applications.

In order to overcome these problems and keep a stable flame front while increasing pressure, Helium can be used as a diluent. This method has been widely used in the literature [3,10,11]. Indeed, this species allows to artificially increase the thermal diffusivity, He having a very high thermal conductivity. The drawback of this technique being that a mixture highly diluted in Helium tends to dissipate the energy very fast which makes ignition more difficult. Moreover, the heat losses

occurring at the end of the propagation (i.e. when the flame approaches the wall) may be notably affected.

One of the main difficulties in SEF-CONV experiments is to identify the limits of the usable data range in order to determine S_u. Indeed, at the beginning of propagation the flame is affected by stretch effects (low-pressure limit) whereas at the end, wall heat loss affects the isentropic compression hypothesis (high-pressure limit). Being outside those limits means the main hypotheses allowing to derive Eq. 1 are not valid anymore. Hence, a comprehension of these phenomena is critical for a good determination of S_u. Figure 2 represents the simultaneous evolution of R_f and P over time. The reasonable zone for S_u extraction is labeled as the 'isochoric conditions' zone.

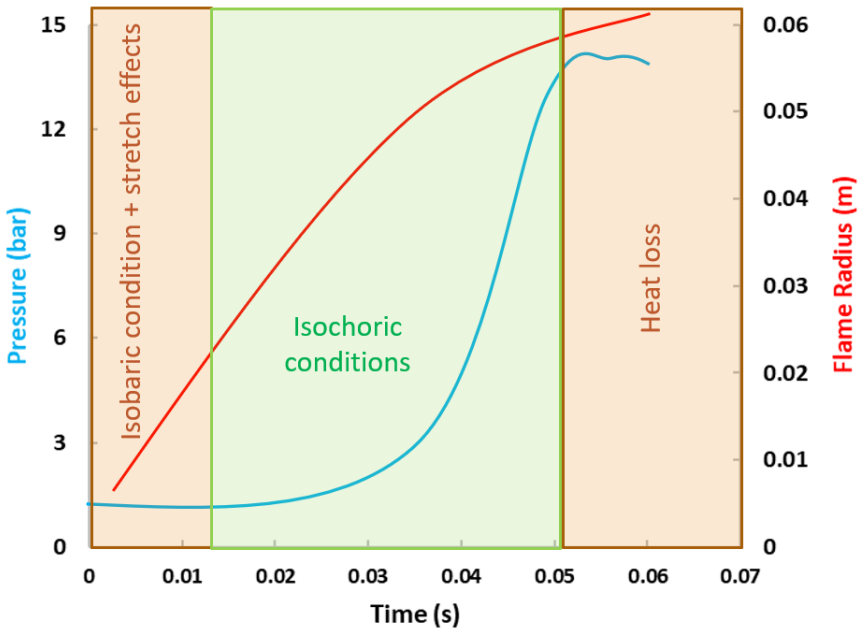

Figure 2: Flame speed determination range

Concerning the low-pressure limit, the stretch of the spherical flame is evaluated as $\mathrm{K} = \frac{2}{R_f}\left(\frac{dR_f}{dt}\right)$. It has been demonstrated in by assessing the contribution of the different sources of inaccuracy that stretch effect can be neglected for pressures greater than 2 times the initial pressure P_0. Concerning the high-pressure limit, an initial criterion of 90% max$(\frac{dP}{dt})$ was defined in [3,9] according to DNS calculations performed for different CH_4/Air mixtures, but this criterion will be reevaluated in this study.

The objective of this paper is to revisit the criteria available to describe the heat exchanges of a premixed flame propagating perpendicular to a wall. In internal combustion systems, it is essential to evaluate heat losses as a function of the flame-wall distance [4,12]. Our specific objective is to develop a criterion to ensure that the flame speed evaluation in SEF-CONV is performed under adiabatic conditions.

To achieve these goals, 1D direct numerical simulations were performed to evaluate the effect of heat losses on the flame dynamics for a large range of mixture conditions.

The in-house code A-SURF [13–15] is used to simulate the 1D spherical expanding flame in a closed chamber with radius of 6.085 cm. The computational domain was initially filled with static mixture at the specified initial pressure and temperature. The spherical flame propagation was initiated by a hot

spot at the center with a small diameter so that its composition and energy content would not affect the computed S_u. Zero flow speed and zero gradients for temperature and mass fractions are enforced at both the center and the wall. In A-SURF, the fully compressible Navier-Stokes equations for a multi-component reactive mixture in 1D spherical coordinates are solved using the finite volume method. The detailed chemistry and transport are considered. The thermal diffusion and radiation are neglected. The FFCM-1 mechanism [16] are used for methane oxidation. The chemical kinetics as well as the thermodynamic and transport coefficients are handled by CHEMKIN [17] and TRANSPOT [18] packages. To accurately and efficiently resolve the flame front, the locally and dynamically adaptive mesh refinement (AMR) technique is also applied based on the gradient of temperature. A 6-level AMR with the finest mesh size of 9.5 µm is initially adopted, and the maximum mesh level will increase 1 level once the end gas pressure is doubled. In this way, the flame fronts are covered by adequate meshes and the gird convergence is ensured. A-SURF has been successively applied in previous studies on outwardly propagating spherical flame [13,14,19,20]. The details on numerical methods and schemes of A-SURF can be found in Refs [13–15]. and thereby are not repeated here. These results will be very useful to propose a new adiabaticity criterion (high pressure limit).

2. Wall effects on the flame speed: definition of a new criterion

In order to validate the new criterion, DNS calculations were performed with the A-SURF code with either adiabatic or isothermal wall condition. In order to compare the new high-pressure limit, some criteria used by other teams on their own SEF-CONV experiments have been listed in the following table.

Table 1: high-pressure criteria from the literature

Source	Criterion
Halter [2,9]	90% max $(\frac{dP}{dt})$ – for safety margin 5 $\frac{P}{P_0}$
Omari/Tartakovsky [21]	max $(\frac{d^2P}{dt^2})$ – for safety margin $Pr = \frac{P-P_0}{P_{eq}-P_0} \sim 55\%$ *
Burrell [5]	max $(\frac{d^2P}{dt^2})$
Razus [22]	max $(\frac{dP}{dt})$

* P_{eq} corresponds to the adiabatic isochoric equilibrium combustion pressure.

Table 2 illustrates that pressure and its derivatives are the main indicators used for heat losses at the wall. Indeed, the evolution of $\frac{dP}{dt}$ over time follows a steep decrease when the heat losses happen.

However, it is still interesting to understand the underlying physical phenomena of the time heat losses appear and, if possible, define a criterion based on these observations. Then, obtained results will be compared to the ones from previous studies for different mixture conditions.

2.1 Laminar flame propagation dynamics and structure

The propagation of laminar flames observed in SEF-CONV experiments is made through the simultaneous compression of the fresh gases and the heating of those gases through thermal diffusion. Once the fresh gases near the flame front reach the ignition temperature, they react and will then heat the nearest fresh gases by diffusion, propagating the phenomenon. Only heat transfers by conduction are considered. Radiation effects can be neglected for several reasons:

- the characteristic time of the flame (i-e the time taken by the flame to travel a distance equivalent to its own thickness δ_f) is negligible compared to the one of radiation heat transfer
- radiations emitted by the burnt gases do not impact the fresh gases which are considered as an optically thin environment
- the fuel used in this study (CH_4) does not lead to combustion products that radiate a lot considering its low number of carbon atoms

Neglecting radiative heat losses in classical SEF-CONV experiments could lead to errors in S_u evaluation (up to 15% according to [23]). However, the advantage of the OPTIPRIME is its optical access, allowing to directly measure R_f. Hence, the radiation effects are implicitly accounted for during S_u calculations. In addition, DNS calculations were performed with A-SURF to assess the importance of radiative heat losses [9]. Simulations show that the adiabatic model gives results very close to the *Statistical narrow band model* (SNB) accounting for radiation emission and reabsorption for conditions similar to the current study. Hence radiative heat losses can be neglected for the studied conditions, confirming the previously listed points.

An interesting aspect of the system composed by the laminar flame and the fresh gases is its structure, composed of three zones of interest illustrated on Figure 3. First, there is the reaction zone of a given width, δ_f. In front of it is a zone called the 'preheating zone' characterized by its thickness (δ_{ph}). This is the zone where the fresh gases near the flame front will be heated until they reach the ignition temperature (T_{ign}) and allow the flame to propagate further. The last zone is found near the wall. It is called the thermal boundary layer (δ_w). Here, the wall is considered as isothermal and acts as a heat sink. Therefore, a temperature gradient appears and develops over time between the gas and the surface of the combustion chamber.

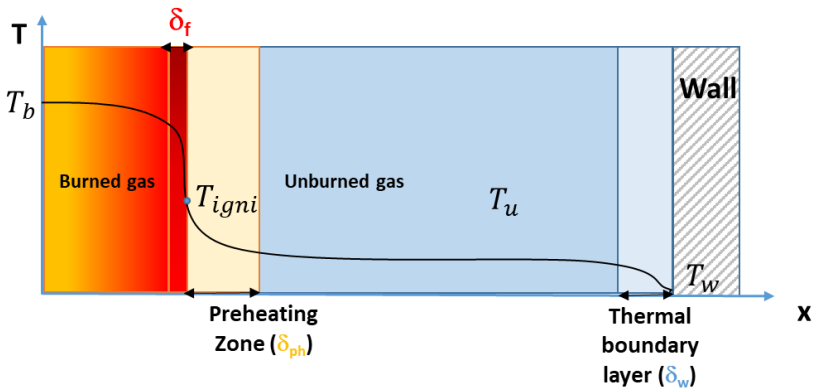

Figure 3 : Illustration of a premixed laminar flame structure

From a phenomenological point of view, the time when the preheat zone (δ_{ph}) and the thermal boundary layer (δ_w) meet and overlap can be considered as the time when the flame starts to lose heat at the wall. Thus, it is interesting to study the evolution of the preheat zone thickness over time.

A power balance on the total power given by the flame $\dot{Q_{tot}}$, to the burnt gases, $\dot{Q_b}$, and to the fresh gases, $\dot{Q_u}$, can be made. It is important to notice that a fraction of $\dot{Q_u}$, noted $\dot{Q_{u_{eff}}}$, will effectively heat the fresh gases while the other part of the power, $\dot{Q_w}$, will be given to the wall. Hence, it is possible to write that the overall power given by the flame can be decomposed as follows, as illustrated in Figure 4:

$$\dot{Q_{tot}} = \dot{Q_u} + \dot{Q_b} = \dot{Q_{u_{eff}}} + \dot{Q_w} + \dot{Q_b} \tag{4}$$

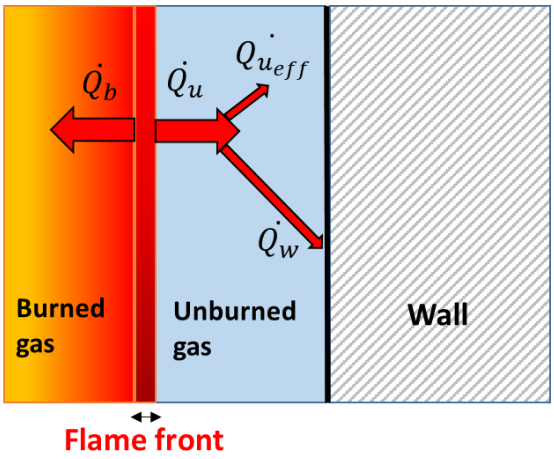

Figure 4: Illustration of the laminar flame power balance

This model supposing homogeneous properties in the unburnt gas and a very thin flame thickness, δ_f.

The power given to the fresh gases decomposes as the product of the gas density ρ_u, heat capacity C_{p_u}, the flame speed S_u and surface times the temperature difference between the unburnt mixture and the flame:

$$\dot{Q_u} = \rho_u \cdot C_{p_u} \cdot S_u \cdot (T_f - T_u) \cdot 4\pi R_f^2 \tag{5}$$

The power given to the wall by conduction is expressed as follows:

$$\dot{Q_w} = \lambda_u \cdot \frac{dT}{dr} \cdot 4\pi R_{tot}^2 \tag{6}$$

A code has been developed to compute the fresh gas parameters over time knowing the pressure during the experiment and the initial conditions (mixture composition and initial P and T). This tool is based on all the above-mentioned hypotheses (ideal gas, isentropic compression, homogeneous parameters in the gases) and the FFCM1 thermodynamic database [16]. Hence, it is possible to know the evolution of $T_u, \rho_u, \lambda_u, C_{p_u}$ and thermal diffusivity $D_{th,u}$ over time. Knowing S_u, it is now possible to compute the power given to the fresh gases and to the wall, but these quantities do not lead to a viable criterion since they rely on the initial conditions.

2.2 Preheating zone thickness evolution and high-pressure limit criterion

In order to evaluate the preheating zone thickness, δ_{ph}, the definition given by Gaydon and Wolfhard was used. δ_{ph} is thus defined as the product between a scalar A (which numerical value will be

discussed in the next section) and the flame thickness, δ_f, from Zeldovitch definition as shown in Eq. 6:

$$\delta_{ph} = A \cdot \frac{\lambda_u}{\rho_u \cdot C_{pu} \cdot S_u} \tag{7}$$

Eq. 6 was derived analytically, leading to a coefficient $A = 4.6$. The preheating zone was defined as the zone between the ignition temperature T_{igni} and the fresh gas temperature T_u plus 1 %. With the code mentioned in the previous section, the numerical evaluation of δ_{ph} over time can be performed.

During the combustion process, when the flame radius increases, so does the total power given by the flame, $\dot{Q_{tot}}$. This leads to an increase of P and ρ in the fresh gases, hence a decrease of δ_{ph} over time (λ_u and C_{pu} do not vary much with pressure). At some point, the flame will be close enough to the wall and will start to lose energy. At that moment, the flame speed, S_u, will decrease and δ_{ph} will start to increase. This behavior defines the exact moment when the flame starts to lose power at the wall, i.e. the point where the adiabatic hypothesis is not valid anymore. The criterion is defined as the minimum of δ_{ph} over time. This minimum indeed coincides with the moment when the preheating zone and the thermal boundary layer at the wall start to overlap according to numerical evaluations made thanks to the thermal properties code. This behavior is illustrated in Figure 5.

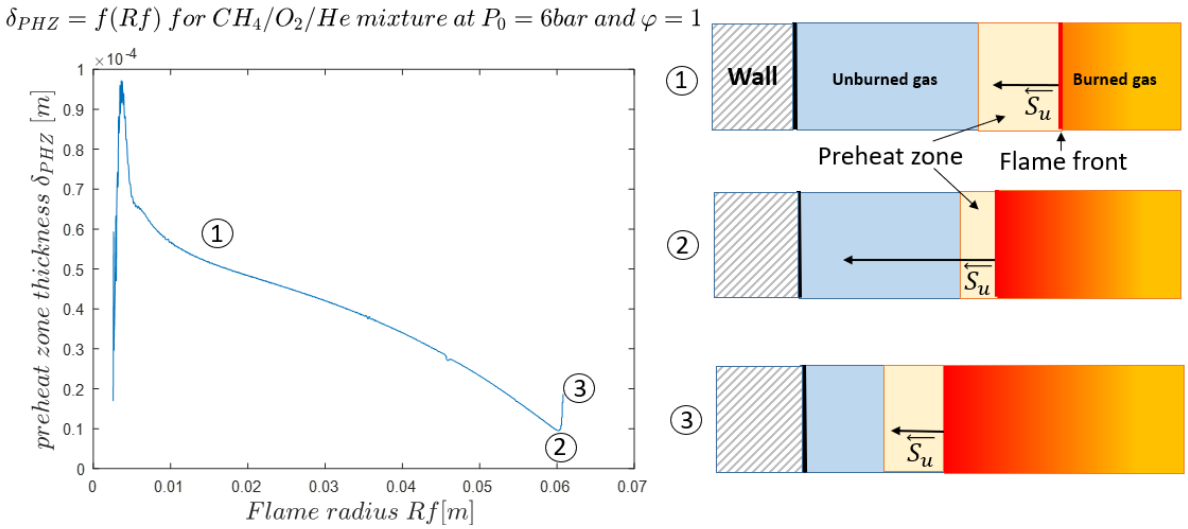

Figure 5: Preheating zone dynamics over time

The computation of δ_{ph} supposes that the flame speed S_u has already been computed on a broad pressure domain. Therefore, the determination of the upper pressure criterion and the truncation are made afterwards. The computation of the thermodynamics parameters involved in the criterion definition is made with the help of the fresh gas parameters computation code described in the previous section.

2.3 Robustness of the new criterion

To test the criterion's robustness over a wide range of S_u (from 0.11 to 1.34 m s^{-1}), δ_f (from 4.8x10^{-5} to 2.11x10^{-4}m) and D_{thu} (from 1.3x10^{-6} to 4.7x10^{-5} m^2. s^{-1}), different mixtures for different initial conditions were considered (see Table 2):

Table 2: Tested mixtures

Mixtures	φ	P_0 (bar)	T_0 (K)
CH_4/air	1.1	1-3-6	300
	1.3	1-3-6	300
CH_4/ 15%O_2 85%He	1.1	1-3-6	300
	1.3	1-3-6	300

The new criterion is defined as the minimum of δ_{ph}. This definition relies on a constant value of A (the ratio between the preheating and the reaction zone) whatever the mixture conditions are during the flame propagation. This point needs to be assessed. In order to numerically evaluate A , the δ_{ph} over δ_f ratio has been computed for a large range of conditions. 1D flame speed calculations were performed using the PREMIX package from CHEMKIN. S_u was computed for the initial conditions of Table 2 and for each case, 3 successive *P* and *T* conditions along the isentropic compression were selected to evaluate the evolution of A during the flame propagation. On the average of the tested conditions, the A value was around 5.

As mentioned previously, δ_{ph} is defined between T_u+1% and T_{igni}, the latter being difficult to evaluate. The temperature corresponding to the position where 5% of the unburnt fuel mass fraction is consumed was arbitrary considered as T_{igni}.

The main conclusion of this evaluation is that the ratio between the thicknesses of the preheating zone and the reaction zone, even if not strictly equal to 4.6, does not vary quantitatively during the flame propagation for a given definition of T_{igni}, confirming that the proposed definition is a robust criterion of adiabaticity. Furthermore, since the method focuses on the minimalization of the δ_{ph} parameter and that it has been proven that A is constant during flame propagation, the value of the coefficient does not matter much as it will not impact the position of min(δ_{PH}).

2.4 Evaluation of the new criterion performance

In this section, DNS using A-SURF are used to check how the proposed criterion (minimum of δ_{ph}) performs to indicate the time when the flame starts to lose power at the wall and that the isentropic compression hypothesis vanishes. Calculations of S_u were performed with either adiabatic ($S_{u\,adi}$) or isothermal ($S_{u\,isoth}$) wall for the conditions of Table 2. As mentioned before, radiative losses are not considered. The relative difference between $S_{u\,adi}$ and $S_{u\,isoth}$ was monitored during the flame propagation. At some point $S_{u\,isoth}$ drops while $S_{u\,adi}$ continues to increase, indicating the point where heat losses occur, as illustrated in Figure 6.

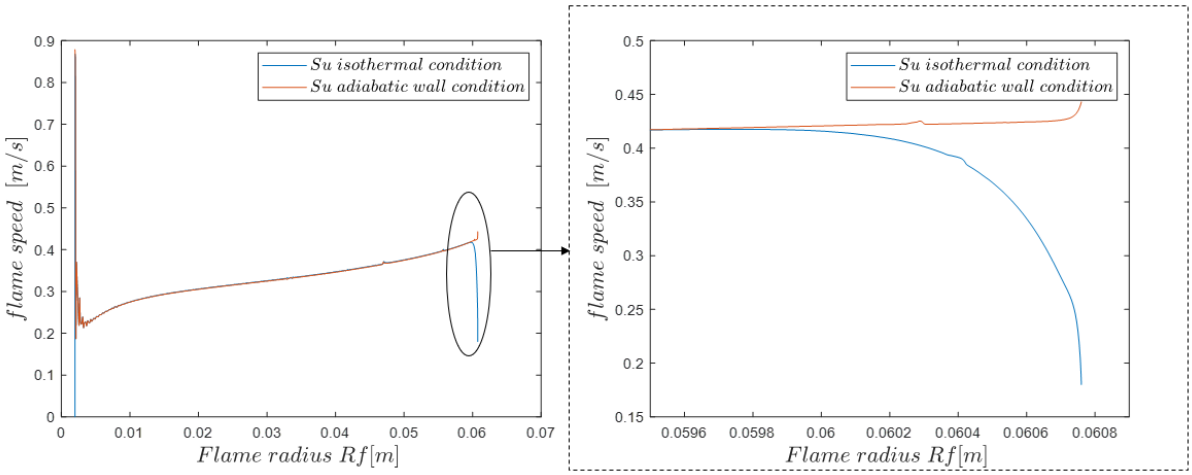

Figure 6: Flame speed evolution as a function of the flame radius. Adi wall in orange and isoT in blue. Mixture is CH_4/Air at φ=1.1 and P_0=1 bar

A relative difference of 5% on the DNS flame speeds, equivalent to the experimental uncertainty of OPTIPRIME [9], was chosen as the DNS criterion to point out this high-pressure limit. However, it is possible to be more accurate in terms of end of adiabaticity hypothesis, considering a lower relative difference on S_u. Nevertheless, the general idea of SEF-CONV setups is to obtain S_u data corresponding to the highest possible pressure. Indeed, as illustrated in Figure 7, the last instants of the flame propagation cover the higher pressure rise. This figure illustrates the flame-wall distance evolution as a function of pressure and clearly exhibits that the higher pressure increase is achieved during the latest millimeters.

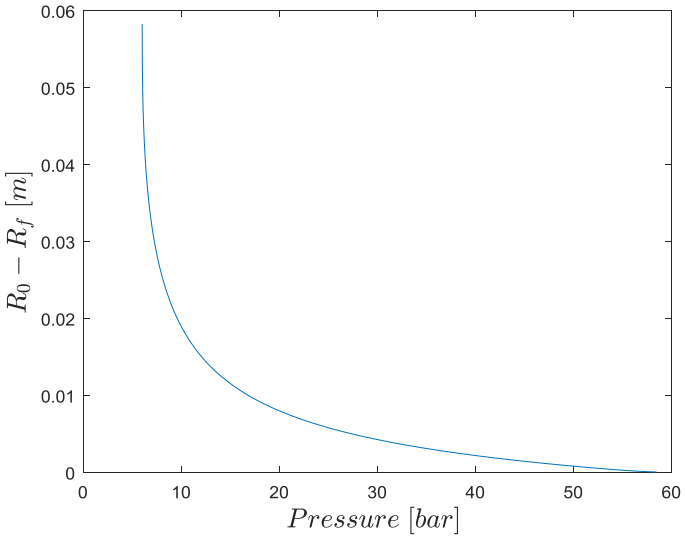

Figure 7: Variation of the flame-wall distance with pressure. Mixture is $CH_4/O_2/He$ at φ=1.1 and P_0=6 bar

Hence, in order to maximize the amount of high-pressure data considered at the end of the experiment while remaining in the setup margin of error, the 5% relative difference on the DNS flame speed was chosen as the numerical benchmark in this study. The balance between accuracy and maximal pressure reached is shown in Figure 8.

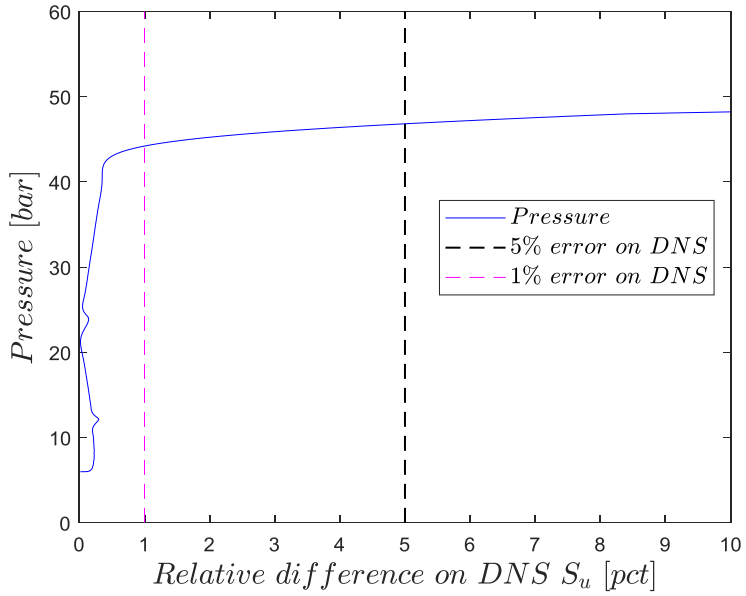

Figure 8: Pressure evolution over relative difference between $S_{u\,adi}$ and $S_{u\,isoth}$ numerical flame speeds. Mixture is methane/air at $\varphi = 1.3$, $P_0 = 6\ bar$

Figure 9 highlights the clear correlation between the DNS and the δ_{PH} criterion. Indeed, the 5% error on the numerical S_u and the minimum of the preheat zone are extremely close to each other (0.12% of relative difference in the case of Figure 8). This observation is valid for the scope of the tested conditions chosen to vary the S_u, D_{th} and δ_f parameters presented in Table 2. Indeed, on average, the relative difference between the two criteria is < 0.15%. Those values tend to confirm the validity of the δ_{ph} criterion from a physical point of view, at least for CH_4/air or $CH_4/O_2/He$ mixtures.

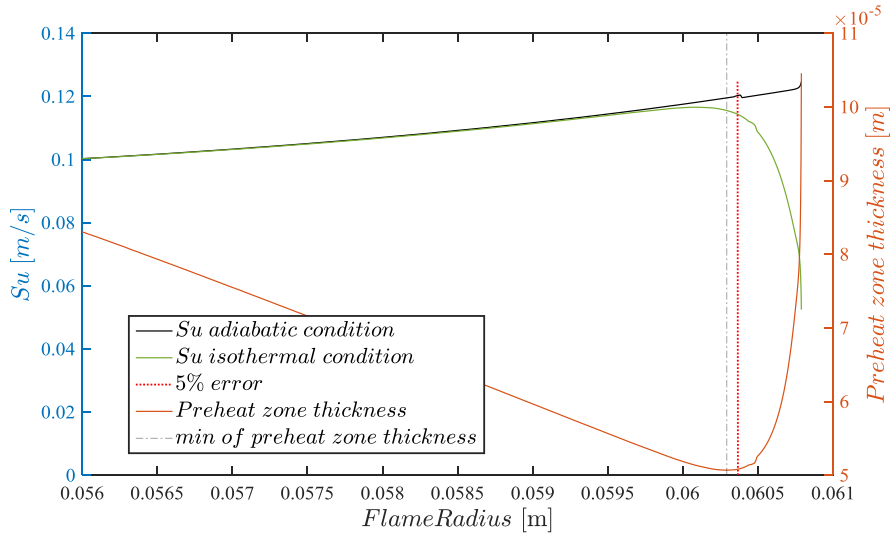

Figure 9: DNS criterion vs. preheat zone thickness criterion. Mixture is methane/air at $\varphi = 1.3$, $P_0 = 6\ bar$

3. Comparison with other criteria

As indicated in Table 1, the majority of the high-pressure limit criteria are based on the pressure evolution. It is now possible to compare the values used by those methods to our new proposed criterion and to test their performances using DNS results. Figure 10 shows the critical flame radii R_{crit} found by the criteria presented in Table 2 for methane/air mixture at φ = 1.3 and P_0 = 1 bar. It illustrates the fact that all the R_{crit} are relatively close to each other but that the critical radius can be over or underestimated depending on the conditions. This observation remains true regardless of the conditions listed in Table 2. This highlights the need for a robust and precise criterion allowing to reach the highest pressures while considering the physical phenomenology of the flame behavior.

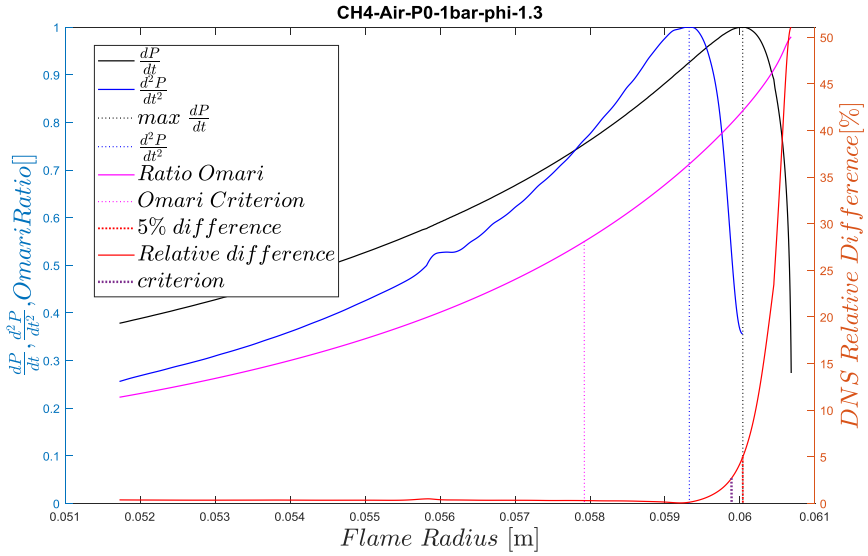

Figure 10: Critical radii of criterion from different studies. Mixture is methane/air at $\varphi = 1.3$, $P_0 = 1\ bar$

Knowing the R_{crit} from all criteria for the conditions of Table 2, it is possible to compare their relative differences with the set DNS criterion of 5% gap between $S_{u\ adi}$ and $S_{u\ isoth}$ in order to assess their accuracy and robustness. It is important to notice that some conditions of Table 2 are missing because the DNS calculations did not converge.

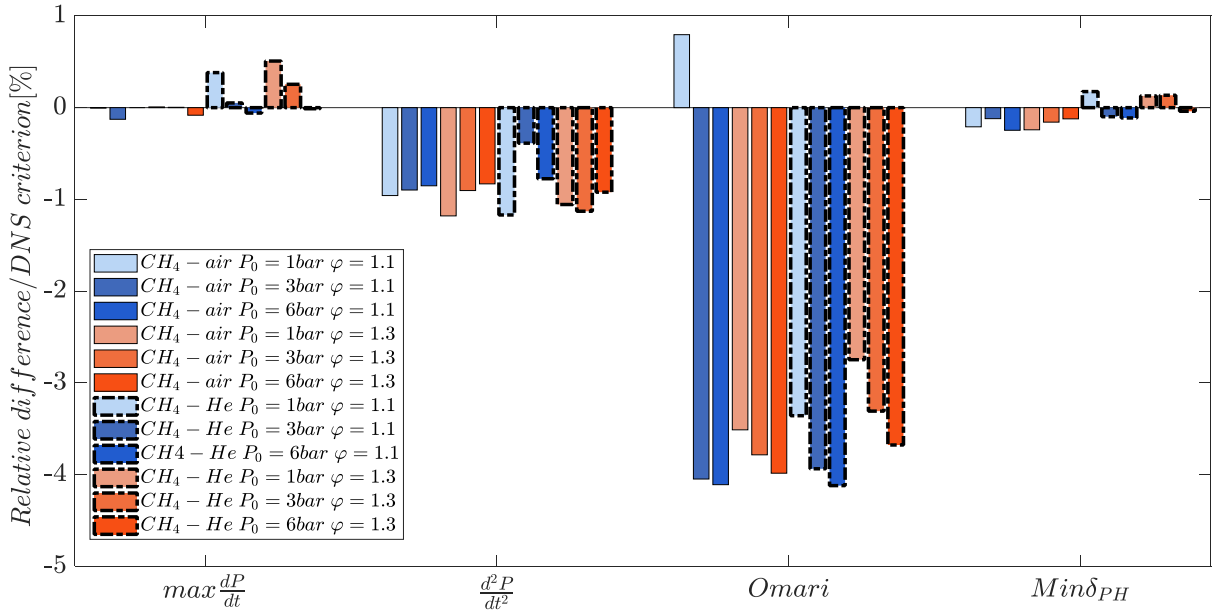

Figure 11 : Relative difference between critical radius criteria and DNS criterion (5% relative difference between $S_{u\ adi}$ and $S_{u\ isoth}$)

Figure 11 allows drawing multiple conclusions:

- Among all the evaluated criteria, min (δ_{ph}) seems to be the most accurate compared to the set DNS criterion (indeed the relative difference is minimal in almost all conditions).
- Max ($\frac{\partial P}{\partial t}$) is sometimes even more accurate even though it seems to be the case only for CH_4/air mixtures. Indeed, the relative difference with DNS is far greater for CH_4/He mixtures. Hence min (δ_{ph}) seems to better consider the diluent effect (modification of D_{th}) on the flame dynamics.
- Max ($\frac{\partial^2 P}{\partial t^2}$) and *Omari* criteria seem both to systematically underestimate the critical radius. However, this observation is consistent with the aim of Omari and Tartakovsky study being a compromise between the limit accuracy and the available data range.

The evaluation of the standard deviation, σ, for each criterion compared to DNS gives additional information. Table 3 allows evaluating the criterion consistency for the scope of tested conditions regarding the set DNS criterion.

Table 3: Standard deviation of criteria for 5 %DNS criterion

$\boldsymbol{\sigma_{\frac{\partial P}{\partial t}}}$	$\boldsymbol{\sigma_{\frac{\partial^2 P}{\partial t^2}}}$	$\boldsymbol{\sigma_{Omari}}$	$\boldsymbol{\sigma_{\delta_{PH}}}$
0.1970	0.2157	1.3572	0.1469

Note that these observations are made for the chosen DNS criterion of 5% and could change if another percentage, for example lower than 5%, was chosen. The data reveals that max ($\frac{\partial^2 P}{\partial t^2}$) is as consistent as min (δ_{ph}). Two conclusions can be drawn from this observation:

- Min (δ_{ph}) criterion is comforted as a robust and precise criterion for the OPTIPRIME target conditions.
- Max ($\frac{\partial^2 P}{\partial t^2}$) is a secure and robust criterion that can be used as a good compromise between the accuracy of the end of adiabaticity limit and the available data range.

As mentioned in section 2d, it is possible to take a lower relative difference on the DNS flame speeds as a reference criterion for the end of adiabaticity regime in order to be more precise. This can be done assuming that the experimental measurements are accurate enough. Indeed, in the case of OPTIPRIME, the general idea of the 5% difference on DNS S_u is to stay in the setup margin of error while maximizing the amount of high-pressure data considered. If a DNS criterion of 1% relative difference between $S_{u\ adi}$ and $S_{u\ isoth}$ is now considered, the previous criteria comparison is also reevaluated as shown on the figure below, and several observations can be made.

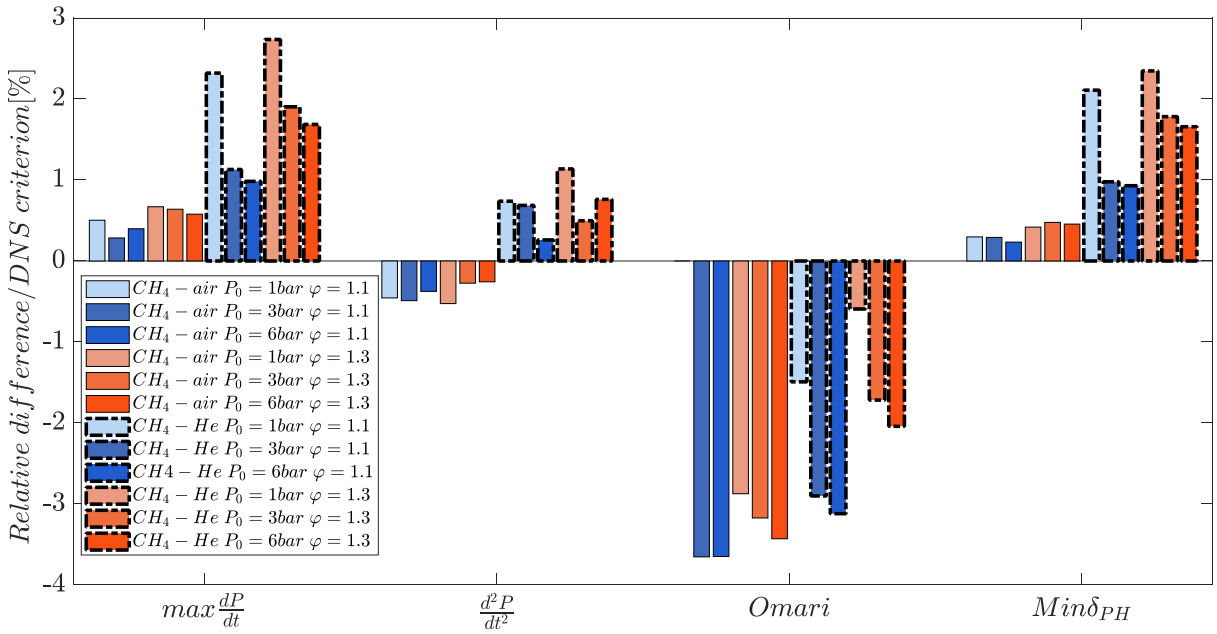

Figure 12 : Relative difference between critical radius criteria and DNS criterion (1% relative difference between $S_{u\ adi}$ and $S_{u\ isoth}$)

The standard deviation was also derived to give additional information concerning the robustness of the different criteria (Table 4):

Table 4: Standard deviation of criteria for 5%DNS criterion

$\boldsymbol{\sigma_{\frac{\partial P}{\partial t}}}$	$\boldsymbol{\sigma_{\frac{\partial^2 P}{\partial t^2}}}$	$\boldsymbol{\sigma_{Omari}}$	$\boldsymbol{\sigma_{\delta_{PH}}}$
0.8155	0.6005	1.4779	0.7738

- It appears that considering a lower percentage for the DNS criterion does not affect that much *Omari*'s behavior while the accuracy of the others is highly impacted. Hence, by always underestimating the critical radius for different reference criteria, *Omari* can be seen as a secure observation when a compromise between the accuracy limit and the available data range needs to be made. However, it remains the less stable criterion of this study, as far as standard deviation is concerned.
- Max ($\frac{\partial^2 P}{\partial t^2}$) does not seem to systematically underestimate the critical radius anymore since it overpredicts it principally for CH_4-He mixtures. It is, however, important to notice that it gives very accurate data in this case.
- Max ($\frac{\partial P}{\partial t}$) and min ($\delta_{ph}$) seem to have a similar behavior, as they both overestimate the critical radius globally by the same factor. It is interesting to notice that the overestimation is more important for CH_4- He cases. However, even if their global standard deviation is impacted, they still give accurate data for CH_4-Air mixtures with less than 1% relative difference with DNS.

Hence, it seems that, when considering a low percentage DNS criterion, the limit of adiabaticity regime is more difficult to evaluate for CH_4- He cases.

The choice of this reference criterion needs to be done accordingly to the studied mixture and to the main objective of the measurement, i.e. to find a balance between maximizing the number of high-pressure data and being secure enough on the available experimental data range.

4. Conclusion

The use of the Spherical Expanding Flame at Constant Volume method provides a large amount of accurate data for a wide range of pressure and temperature. One limitation relies on the perfect sphericity of the flame during the whole process. Helium dilution is a solution to push back the limits of cellularity occurrence on the flame surface.

When the flame front approaches the wall, heat exchanges increase. They are favored when the thermal diffusivity of the mixture is high. The objective of this paper is to propose a model allowing to identify the conditions for which the propagation of the flame can be considered adiabatic.

A new criterion based on the minimization of the preheating zone thickness has been defined. Its robustness and its performance have been assessed.

It is possible to affirm that min (δ_{ph}) is a well-optimized criterion for the extraction of high-pressure S_u. Indeed, it has shown very good results with respect to the 5% difference reference criterion on DNS calculations. Considering the other criteria, the pressure first derivative and Omari criteria clearly have an inferior precision for the 5 and 1% difference reference criterion on DNS results. The max ($\frac{\partial^2 P}{\partial t^2}$) criterion, however, is the most precise for the latter reference condition. Hence, 2 criteria have been identified as robust and precise tools to identify the end of adiabaticity limit, relatively to its definition.

The other advantage of the min (δ_{ph}) criterion is that it is based on a phenomenological approach of the flame behavior directly accounting for the mixture composition. The results proved to be coherent with the overlap of the preheat and thermal boundary layer zones, confirming the physical interpretation of the end of adiabaticity. Hence, it is possible to have reliable data even for mixtures

composed of high percentages of helium (increasing the D_{th} and thus decreasing the value of R_{crit} compared to CH_4/air conditions). It is also important to note that min (δ_{ph}) can be adapted to process data coming from every experimental SEF-CONV setups. Hence, it is possible to find a balance between the upper pressure limit accuracy and the range of available data.

Fundings

This research did not receive any specific grant from funding agencies in the public, commercial, or not-for-profit sectors.

Declaration of competing interest

The authors declare that they have no known competing financial interests or personal relationships that could have appeared to influence the work reported in this paper.

References

[1] B. Lewis, G. Von Elbe, Determination of the speed of flames and the temperature distribution in a spherical bomb from time-pressure explosion records, J. Chem. Phys. 2 (1934) 283–290.

[2] F. Halter, G. Dayma, Laminar flame speed determination at high pressure and temperature conditions for kinetic schemes assessment, in: Proc. Combust. Inst., 2020.

[3] A. Movaghar, R. Lawson, F.N. Egolfopoulos, Confined spherically expanding flame method for measuring laminar flame speeds: Revisiting the assumptions and application to C1C4 hydrocarbon flames, Combust. Flame. 212 (2020) 79–92.

[4] M.M. Elia M., Laminar burning velocity of methane-air-diluent mixtures, J. Eng. Gas Turbines Power. 123 (2001) 190–196.

[5] R.R. Burrell, J.L. Pagliaro, G.T. Linteris, Effects of stretch and thermal radiation on difluoromethane/air burning velocity measurements in constant volume spherically expanding flames, Proc. Combust. Inst. 37 (2019) 4231–4238.

[6] Y. Yamamoto, T. Tachibana, Burning velocities of dimethyl ether (DME)–nitrous oxide (N2O) mixtures, Fuel. 217 (2018) 160–165.

[7] N. Hinton, R. Stone, R. Cracknell, Laminar burning velocity measurements in constant volume vessels – Reconciliation of flame front imaging and pressure rise methods, Fuel. 211 (2018) 446–457.

[8] M. Faghih, Z. Chen, The constant-volume propagating spherical flame method for laminar flame speed measurement, Sci. Bull. 61 (2016) 1296–1310.

[9] F. Halter, Z. Chen, G. Dayma, C. Bariki, Y. Wang, P. Dagaut, C. Chauveau, Development of an optically accessible apparatus to characterize the evolution of spherically expanding flames under constant volume conditions, Combust. Flame. 212 (2020) 165–176.

[10] G. Rozenchan, D.L. Zhu, C.K. Law, S.D. Tse, Outward propagation, burning velocities, and chemical effects of methane flames up to 60 ATM, Proc. Combust. Inst. 29 (2002) 1461–1470.

[11] G. Wang, Y. Li, W. Yuan, Y. Wang, Z. Zhou, Y. Liu, J. Cai, Investigation on laminar flame propagation of n-butanol/air and n-butanol/O2/He mixtures at pressures up to 20 atm, Combust. Flame. 191 (2018) 368–380.

[12] L. Pizzuti, C.A. Martins, L.R. Dos Santos, D.R.S. Guerra, Laminar Burning Velocity of Methane/Air Mixtures and Flame Propagation Speed Close to the Chamber Wall, Energy Procedia. 120 (2017) 126–133.

[13] Z. Chen, M.P. Burke, Y. Ju, Effects of Lewis number and ignition energy on the determination of laminar flame speed using propagating spherical flames, Proc. Combust. Inst. 32 I (2009) 1253–1260.

[14] Z. Chen, M.P. Burke, Y. Ju, Effects of compression and stretch on the determination of laminar flame speeds using propagating spherical flames, Combust. Theory Model. 13 (2009) 343–364.

[15] P. Dai, Z. Chen, Supersonic reaction front propagation initiated by a hot spot in n-heptane/air mixture with multistage ignition, Combust. Flame. 162 (2015) 4183–4193.
[16] G.P. Smith, Y. Tao, and H. Wang, Foundational Fuel Chemistry Model Version 1.0 (FFCM-1), http://nanoenergy.stanford.edu/ffcm1, 2016., (n.d.).
[17] R.J. Kee, F.M. Rupley, J.A. Miller, Chemkin-Ii: a Fortran Chemical Kinetics Package for the Analysis of Gas-Phase Chemical Kinetics, J. Chem. Inf. Model. 53 (1989) 1689–1699.
[18] R.J. Kee, sss A FORTRAN COMPUTER CODE PACKAGE FOR THE EVALUATION OF GAS-PHASE,MULTICOMPONENT TRANSPORT PROPERTIES, J. Chem. Inf. Model. 53 (2013) 1689–1699.
[19] Y. Wang, A. Movaghar, Z. Wang, Z. Liu, W. Sun, F.N. Egolfopoulos, Z. Chen, Laminar flame speeds of methane/air mixtures at engine conditions: Performance of different kinetic models and power-law correlations, Combust. Flame. 218 (2020) 101–108.
[20] Z. Chen, On the accuracy of laminar flame speeds measured from outwardly propagating spherical flames: Methane/air at normal temperature and pressure, Combust. Flame. 162 (2015) 2442–2453.
[21] A. Omari, L. Tartakovsky, Measurement of the laminar burning velocityusing the confined and unconfined spherical flame methods - A comparative analysis, Combust. Flame. 168 (2016) 127–137.
[22] Razus, Burning Velocity of Propane−Air Mixtures from Pressure−TimeRecords during Explosions in a Closed Spherical Vessel.pdf, (n.d.).
[23] C. Xiouris, T. Ye, J. Jayachandran, F.N. Egolfopoulos, Laminar flame speeds under engine-relevant conditions: Uncertainty quantification and minimization in spherically expanding flame experiments, Combust. Flame. 163 (2016) 270–283.